Anaerobe 41 (2016) 113–124

Contents lists available at ScienceDirect

Anaerobe

journal homepage: www.elsevier.com/locate/anaerobe

Tetanus toxin production is triggered by the transition from amino acid consumption to peptides

Cuauhtemoc Licona-Cassani [a, c, 1], Jennifer A. Steen [a, 1], Nicolas E. Zaragoza [a], Glenn Moonen [b], George Moutafis [b], Mark P. Hodson [a, d], John Power [b], Lars K. Nielsen [a], Esteban Marcellin [a, *]

[a] Australian Institute for Bioengineering and Nanotechnology (AIBN), The University of Queensland, Brisbane, QLD 4072, Australia
[b] Zoetis, 45 Poplar Road, Parkville, VIC 3052, Australia
[c] National Laboratory of Genomics for Biodiversity (LANGEBIO), Cinvestav-IPN, Irapuato, Mexico
[d] Metabolomics Australia Queensland Node, AIBN, The University of Queensland, Brisbane, QLD 4072, Australia

ARTICLE INFO

Article history:
Received 4 April 2016
Received in revised form
27 July 2016
Accepted 27 July 2016
Available online 1 August 2016

Handling Editor: Bruce A McClane.

Keywords:
Clostridium tetani
Fermentation maps
Systems biology
TeTN production

ABSTRACT

Bacteria produce some of the most potent biomolecules known, of which many cause serious diseases such as tetanus. For prevention, billions of people and countless animals are immunised with the highly effective vaccine, industrially produced by large-scale fermentation. However, toxin production is often hampered by low yields and batch-to-batch variability. Improved productivity has been constrained by a lack of understanding of the molecular mechanisms controlling toxin production. Here we have developed a reproducible experimental framework for screening phenotypic determinants in *Clostridium tetani* under a process that mimics an industrial setting. We show that amino acid depletion induces production of the tetanus toxin. Using time-course transcriptomics and extracellular metabolomics to generate a 'fermentation atlas' that ascribe growth behaviour, nutrient consumption and gene expression to the fermentation phases, we found a subset of preferred amino acids. Exponential growth is characterised by the consumption of those amino acids followed by a slower exponential growth phase where peptides are consumed, and toxin is produced. The results aim at assisting in fermentation medium design towards the improvement of vaccine production yields and reproducibility. In conclusion, our work not only provides deep fermentation dynamics but represents the foundation for bioprocess design based on *C. tetani* physiological behaviour under industrial settings.

1. Introduction

Clostridium tetani, the causative agent of tetanus, is an important pathogen of humans and animals. The disease occurs when a wound is infected with vegetative cells or spores which then produce an extracellular neurotoxin (tetanospasmin or TeNT) that blocks inhibitory neurotransmitters in the central nervous system [1]. To date, much of the research on *C. tetani* has been focussed on the mechanism of TeNT [2–6]. More extensive research has been restricted by the absence of reproducible culturing conditions and genetic tools to allow for the study of this organism at the molecular level. To compound this, vaccines are so effective that understanding the organism has not been required to manage disease burden [7].

Worldwide, billions of people and countless companion and production animals are protected from tetanus by immunisation with highly effective TeNT toxoid vaccines. Despite its importance, the current fermentation processes have advanced little since the 1970s. While not reported in scientific literature, industrial TeNT production is hampered by low titres and occasional batch failures (communication, Zoetis Inc.). TeNT is produced from *C. tetani* cultures grown under classical batch fermentation conditions. At the end of the fermentation, after ~150 h, the active toxin is harvested from the culture supernatant. The toxin is subsequently inactivated with formalin before it is mixed with other components for use in multivalent vaccines. The medium used for TeNT production is critical and typically consists of peptides from digested casein, soy or occasionally other plant derived peptones, which are inherently of inconsistent quality. In addition, during medium formulation,

* Corresponding author.
E-mail address: e.marcellin@uq.edu.au (E. Marcellin).
[1] Equal contributors.

http://dx.doi.org/10.1016/j.anaerobe.2016.07.006

medium components also undergo additional poorly-controlled modifications such as calcium precipitation [8–10] and Maillard reactions [11] which exacerbate the variability in yields. Critically, it remains unclear which components of the medium are essential for toxin production and even the fundamental reason(s) for the organism to produce toxin.

Attempts to improve TeNT production using traditional rational process engineering approaches have had limited success [12]. Fed-batch processes that increase cell density and TeNT production have not been transferred to the commercial settings, while attempts to rationally design medium have resulted in reduced TeNT production [13]. To improve TeNT production, it is imperative to better understand the biology of *C. tetani* under industrial conditions; apart from the isolated example that links the tetanus toxin precursor gene, *tetX*, expression to the regulator *tetR* [14], little is known about *C. tetani* physiology and TeTN production elicitors. Typically, toxin production in clostridia is a highly regulated and complex molecular process [15]. In the case of TeNT, the gene encoding TeNT (*tetX*) must not only be expressed and translated, but the resulting proto-toxin (pTeNT) must also undergo proteolytic cleavage before the toxin becomes active [16]. Analysis of *tetX* expression and regulation, and TeNT production and maturation has been heavily reliant on comparative analysis with *Clostridium botulinum* and *Clostridium perfringens*.

To address the challenges associated with TeNT production, here we have performed a systematic study of the behaviour of *C. tetani* during bioreactor fermentations for the production of TeNT using a multi-dimensional biological analysis. Systems biology has been widely adopted for the study of model organisms such as yeast and *E. coli* [17] however, it is not widely used for the study of non-model organisms. Here we performed an in-depth time-course analysis of the fermentation that defines nutrient consumption and a 15 time-point transcriptomics profile dataset to provide a detailed 'transcriptional fermentation atlas' of the process. We have identified distinct growth phases and attribute mechanisms to explain the complex life cycle of *C. tetani* in bioreactors, which are tightly controlled through complex growth phase switches at the transcriptional and translational level. At the molecular level, three 'transcriptional stages' were identified. We believe that this research will underpin future improvements to the production of TeNT and contribute to our global understanding of the central metabolic regulation, pathogenicity, and life cycle of *C. tetani* under industrial conditions.

2. Results

The first step for bioprocess optimisation is the establishment of constant environmental conditions to maintain high reproducibility. To achieve high toxin yields, *C. tetani* needs to be fermented using a complex process under a tightly controlled environment. As opposed to our initial attempts in which large batch to batch variability with poor active toxin recovery was observed in flask fermentations, bioreactors provided highly reproducible results (Fig. 1A).

2.1. C. tetani's growth displays two exponential growth phases: exponential I and exponential II

After establishing reliable fermentations, we sampled the fermenters frequently so as to uncover a previously uncharacterised exponential growth phase followed by a second phase of lower growth rate (Fig. 1A). The fermentation begins with a period of exponential growth (Stage I), characterised by rapid production of biomass ($\mu = 0.24 \pm 0.006\ h^{-1}$), a decrease in pH and an increase in dissolved oxygen (DO) (Fig. 1C) (from 0 to 4.5%) when air is passed through the headspace. Ten hours after the start of the fermentation, cells transition to Stage II, which is characterised by a slower growth rate ($\mu = 0.083 \pm 0.005\ h^{-1}$) for the next 30 h. Growth rates were determined by dry cell weight (DCW) and optical density (OD). During this stage, pH increases to a peak of 7.2 after 25 h of the fermentation start, while DO concentrations remain stable. During Stage III (40 h–70 h) cells undergo a phase of autolysis. At this time, dramatic increases in both pH and DO are observed with pH rising from 7.2 to 8.0 and DO increase from 5% to 70%. Stage IV is the final period of toxin maturation in which the proto-toxin in the supernatant becomes biologically active. Although pTeNT must be in the supernatant following autolysis, the concentration of active toxin does not peak until 120 h, some 48 h after complete lysis is observed.

To characterise the biological process for TeNT production at the molecular level, fermenters were sampled regularly during the four growth stages (Fig. 1). Given the influence of medium composition in TeNT production yields and the lack of data supporting its design, we used a systems biology driven approach to understand the physiological program that governs the behaviour of the *C. tetani* population during fermentation. To this end, time course samples were taken for analysis of medium component consumption, namely free amino acids and vitamins (Fig. 1D and E), metal ions, and casein-derived peptides (Fig. 2A and B). Results were mapped to the fermentation profile to generate a physiological fermentation atlas. It is important to note that due to the inherent nature of the fermentation in complex medium results from the repetitions are similar but not identical. This is particularly true for the proteomics study and for the RNA-seq repeats. Variations are likely due to variability in the proteins digestion prior to MS analysis and the inherent nature of the complex fermentations (see for example ph and pO_2 profile for 5 replicates in Fig. 1C). For clarity and simplicity, most results will focus on the fine kinetic fermentation (the one that contains 15 time points) while results from both fermentations are presented in the figures and described in the text.

2.2. Growth on free amino acids

The transition from the Stage I to Stage II is associated with a depletion of a subset of free amino acids from the medium (Fig. 1D). Analysis examining nutrient consumption indicated complete or almost complete (<10% remaining) consumption of glutamic acid, aspartic acid, asparagine, threonine, serine, histidine, and tyrosine. The fastest decrease in amino acid concentration occurs between the 11 h and 13 h, particularly for histidine, glutamic acid, threonine, and serine. Aspartic acid and asparagine were consumed between 10 h and 20 h and tyrosine was consumed after 30 h. Interestingly, depletion of amino acids correlates with the transition from Stage I to Stage II. Contrarily, the concentration of Ile, Pro and Val increased along the fermentation presumably due to the activity of extracellular peptidases (Supplementary Figs. 1 and 2).

To investigate the nutritional dependence of casein-derived peptides in the fermentation, cells were fermented in a chemically defined medium containing the 20 proteinogenic amino acids plus hydroxy-L-proline, cystine [18] and glucose. The chemically defined medium supports growth at $\mu = 0.69\ h^{-1}$ despite no glucose being consumed. When using the chemically defined medium, cells stop growing after the depletion of aspartate, asparagine, glutamate, serine, histidine, methionine, leucine, lysine, arginine, threonine and glutamine while no toxin production was observed confirming the importance of casein peptides and amino acid metabolism in the *C. tetani* fermentation (Supplementary Fig. 3). Further gene expression analysis confirmed that the gene encoding for *tetX* is essentially not transcribed in CDM (data not shown).

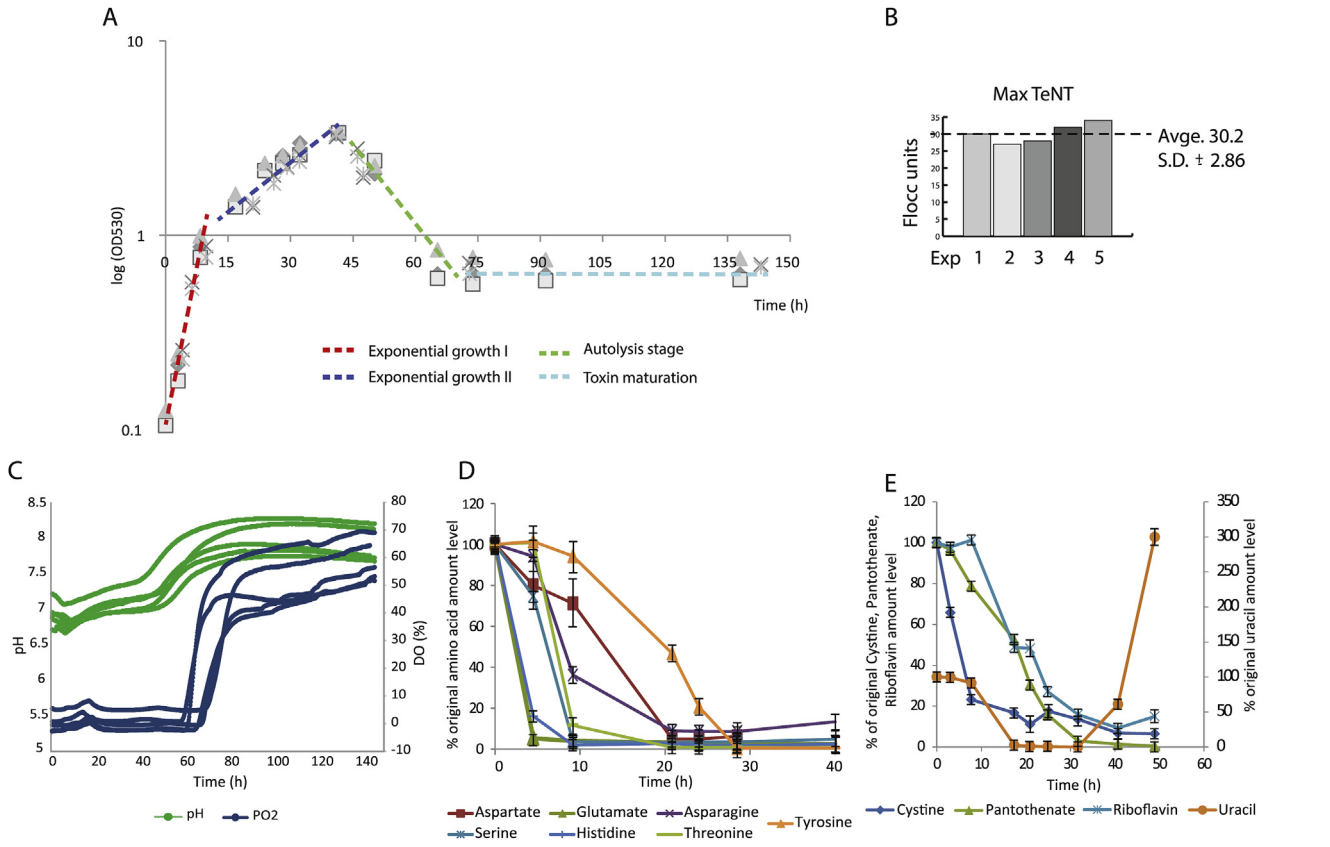

Fig. 1. Characterisation of the bioreactor growth and toxin production during *C. tetani* fermentation. A) Growth characteristics from five independent experiments. The four phases of the fermentation are indicated: exponential growth phase I (Stage I, dashed red), exponential growth phase II (Stage II, dashed blue), autolysis (Stage III, dashed green) and toxin maturation (Stage IV, dashed cyan). B) Concentration of tetanus toxin (TeNT [flocc units]) detected in five independent fermentation supernatants measured approximately 120 h after inoculation. C) pH and pO_2 profiles along the fermentation from five independent experiments D) Temporal dynamics of the free amino acids consumed by *C. tetani* in bioreactor fermentations. Ala, Arg, Gly, Ile, Leu, Lys, Phe, Pro, Trp, Val were not included in the plot as they are not consumed. The concentration of Val, Ile and Pro increases along the fermentation (Supplementary Fig. 2) probably due to peptidase activity. The HPLC quantification method used was unable to quantitate Cys. Error bars represent the standard deviation (SD) of the mean. E) Consumption of vitamins during *C. tetani* fermentation. The data for amino acid and vitamin concentration are represented as percentage of the starting material. Error bars represent the standard deviation (SD) of the mean. Amino acids and metabolomics data represents a typical fermentation run. (For interpretation of the references to colour in this figure legend, the reader is referred to the web version of this article.)

2.3. Casein-derived peptides were consumed during linear growth

After consuming free amino acids during Stage I, cells consume peptides from casein in complex medium triggering the onset of expression of the *tetX* gene (Supplementary Fig. 4). Quantitative proteomics was used to identify the peptides consumed during this stage in two independent fermentations. It is important to note that result vary between the 2 biological replicates, likely due to variations during trypsin digestion of the casein prior to LCMS or due to lot to lot variability in media preparation. Using this approach, we detected consumption of five peptides (VPQLEIVPN, VYPFPGPI, VYPFPGPIPN, KVPQLEIV and YQEPVLGPV) and (KVPQLEIVPN, TQTPVVVPPFLQPEV, TDAPSFSDIPNPI, VYPFPGPIPN and SLPQNIPPLTQTPV). In the first fermentation, consumption dynamics showed that peptide VPQLEIVPN is consumed between 8 h and 18 h, KVPQLIEV is consumed between 8 h and 25 h and peptides YQEPVLGPV, VYPFPGPI and VYPFPGPIPN are consumed between 25 h and 32 h of the fermentation, while in the second biological replicate the peptide KVPQLEIVPN and TQPVVVPPFLQPEV are consumed first (Fig. 2A and B). While peptide consumption and growth behaviour are uncorrelated events, it would appear that the presence of specific peptides is essential for activation of key cellular programs such as the production of TeNT.

2.4. Role of key vitamins, minerals and glucose on the fermentation

Casein provides more than just peptides; at a minimum, vitamins, minerals and trace metals are also present in casein. To measure their influence in growth behaviour and toxin production, a subsection of nutrients added to the medium were also monitored for consumption using LC-MS/MS (Fig. 1E). From this analysis, 10 metabolites were measured. From those, L-cystine, calcium pantothenate, and riboflavin were consumed during stage I of the fermentation. Pyridoxine hydrochloride and nicotinic acid accumulate in the medium. Interestingly, uracil was both consumed and produced during the fermentation. Given that iron (Fe^{2+} and Fe^{3+}) is an essential element for both metabolic and pathogenic functions, extracellular and intracellular iron were also quantified. Iron in the medium seemed to be in excess, so no significant changes were observed during the fermentation time course; however, intracellular total iron (Fe^{2+} and Fe^{3+}) slightly decreased during the second stage of the fermentation.

Other medium components, including glucose and zinc, were also monitored. Only 30% of the glucose is consumed in the first 75 h and zinc levels were relatively stable during the first and second stages of the fermentation and peaked upon completion of lysis.

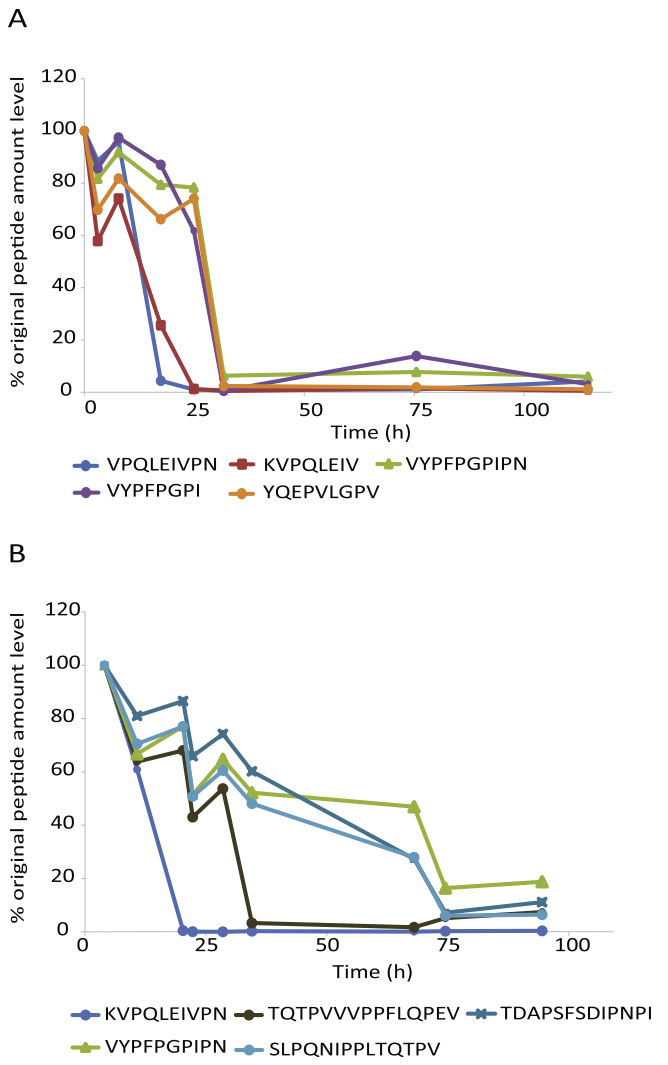

Fig. 2. Relative consumption of the most consumed peptides from casein during *C. tetani* fermentation. Peptide consumption marks the onset of Stage II of the fermentation. The consumption of similar peptides is shown in these figures however, due to abundant sites for trypsin activity it is unlikely to obtain the same peptides for proteomics analysis.

2.5. Analysis of the molecular processes involved in C. tetani fermentation and TeNT production

Unlike the transition between Stage I and II, there is no clear mechanism that can be linked to the transition into Stage III. No correlation was observed between the transition to Stage III and environmental factors such as temperature, dissolved oxygen, redox potential or pH. Remarkably, autolysis was consistently observed 2.3 biomass doubling times after the end of Stage II, irrespective of the initial inoculum and the biomass reached at stage I. This strongly suggests that the onset of autolysis is physiologically determined; therefore, in order to investigate the molecular events underpinning autolysis and toxin production we analysed the transcriptome across the fermentation time course.

2.6. Transcriptomic analysis of the C. tetani fermentation

The in-depth transcriptional analysis was performed to monitor genome-wide transcriptional events from 15 time-points across Stage I and II (Fig. 3A). Transcriptional data were initially assessed by Principal Component Analysis and a clear time-related variance pattern was defined by principal component one (Supplementary Fig. 5A). Subsequently Partial Least Squares/Projection to Latent Structures (PLS) analysis (Supplementary Fig. 5B) and Orthogonal PLS (Fig. 3B) were applied to the data to correlate defined growth stages with transcriptional events across the fermentation. These analyses permit the identification of genes (or groups thereof) that have patterns of expression related to the fermentation time course. For more information relating to these multivariate methods please refer to [19] and [20]. To better understand the physiological conditions driving the various growth stages, transcriptional events linked to the central metabolic pathways and virulence cellular programs were analysed (Fig. 3C).

2.7. Central carbon and energy metabolism

The transcriptional analysis shows that Stage I and II concern primarily ATP generation from amino acid catabolism or peptide degradation. Specifically, genes related to the transport of serine/threonine (*ctc02307*), tyrosine (*ctc00819*), branched chain amino acid (*ctc02088*) and, D-alanine glycine (*ctc01172*) were significantly expressed during Stage I. Similarly, sodium/glutamate symport carrier protein (*ctc02306*) was expressed during the Stage II. Amongst genes coding for enzymes involved in amino acid degradation, the gene for tyrosine phenol-lyase (*ctc00818*) showed high expression during late Stage I and throughout Stage II. In addition, threonine dehydratase (*ctc02624*), L-allo-threonine aldolase (*ctc01037*) and serine dehydratase (alpha and beta subunits, *ctc01981* and *ctc01982*, respectively) coding genes were expressed at Stage I reaching a maximum at Stage II. Remarkably, the glutamate degradation genes methyl-aspartate mutase (*mutS*, *mutE* and *mutL*) together with their transcriptional regulator (*ctc02569*) were only significantly expressed during Stage I, decreasing in expression towards the middle of Stage II. Lastly, the formiminoglutamase coding gene (*ctc01812*), involved in histidine metabolism, was only significantly expressed during early Stage I while aspartate kinase coding gene (*ctc02356*) was only seen to be expressed during Stage II.

Aminotransferases were also significantly expressed along the fermentation time course. For example, serine-pyruvate/aspartate aminotransferase (*ctc00695*) rapidly increased its expression in Stage I and then rapidly decreased at the onset of Stage II. Contrarily, the aspartate aminotransferase (*ctc01294*) and aminotransferase genes (*ctc01359*) had rapid expression during the first 7 h. High expression of four peptidases, namely glutamyl-endopeptidase precursor (*ctc00612*), zinc carboxypeptidase (*ctc00519*), leucyl-aminopeptidase (*ctc01866*) and putative aminopeptidase encoded in the plasmid pE88 (*ctp20*) were also observed during the stage II of the fermentation.

In the pathway for biosynthesis of pyrimidines, the aspartate carbamoyltransferase gene (*ctc02383*) decreased its expression levels at the end of Stage I but increased rapidly by mid- Stage II. Similar expression patterns were observed for uracil phosphoribosyltransferase (*upp*) and the gene encoding the bifunctional pyrimidine regulatory protein PyrR uracil phosphoribosyltransferase (*pyrR*). In the purine biosynthetic pathway, the amidophosphoribosyltransferase gene (*ctc01965*), an enzyme from *de novo* synthesis of purines, showed significant expression during Stage I and II, whereas the phosphoribosyl-formylglycinamidine synthase II gene (*ctc01029*) was only significantly expressed during Stage I. Finally, the genes coding for phosphoribosylaminoimidazole carboxylase catalytic subunit (*ctc01966*), phosphoribosylamine-glycine ligase (*ctc01961*) and phosphoribosyl-aminoimidazole synthetase (*ctc01964*) were evenly expressed along the fermentation.

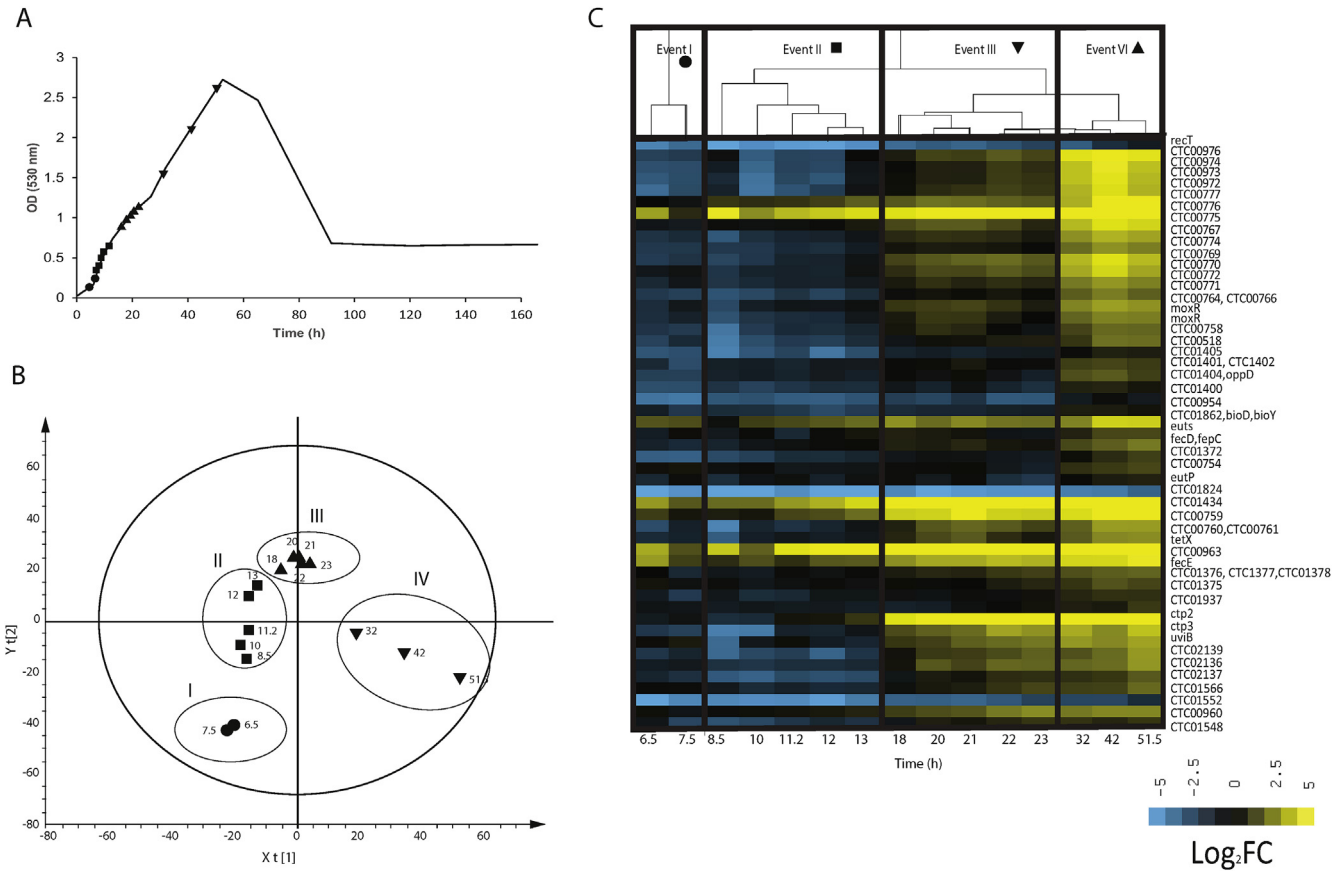

Fig. 3. Overview of the transcriptional molecular map of the *C. tetani* fermentation A) In-depth transcriptional analysis was performed to monitor genome-wide transcriptional events from 15 time-points across the exponential and linear growth phases. RNA-seq data was performed for samples extracted at the times represented by circles, squares, triangles an upside down triangles. The RNA-seq data clusters together in the OPLS analysis by 4 transcriptional clusters as illustrated in B and C. B) Orthogonal Partial Least Squares (OPLS) analysis correlates the growth stages previously defined with 4 transcriptional clusters across the fermentation. Samples from the early stage (6.5 h and 7.5 h) (circles), cluster together. Samples from 8.5 to 13 h (squares), 18–23 h (triangles) and samples 33–52.5 h (upside down triangles) cluster together. Separation of classes is maximised through the predictive component (X-axis), intraclass variability is described through the component (Y-axis). Axis values are arbitrary and relate to the scores derived from the linear combinations of the variables for each observation, providing two-dimensional x and y coordinates for the multivariate data. C) Heat map displaying physiological conditions illustrating the different growth clusters for selected genes clustering near *tet*X; transcriptional events linked to the central metabolic pathways and virulence cellular programs were analysed in depth in Figs. 3–5.

2.8. Iron and ATP metabolism

Three ferrous iron transport coding genes (*ctc00451-00452* and *ctc00534*) were expressed during Stage I and II (Fig. 4A and Fig. 5A). The gene encoding for the iron (III) di-citrate transport system permease protein FecD/HmuV (*fecD*) and the gene coding a hemin transport system ATP-binding protein (*fecE*) were notably higher after the beginning of Stage II and throughout Stage III (Figs. 4B and 5B).

Additionally, Stage I of the fermentation was characterised by high transcription for genes associated with the *rnf* complex, which drives the ATPase synthase in *C. tetani* (Figs. 4C and 5C). The genes associated with ATP synthesis, particularly those linked to (V)-type ATPase synthase (*ctc02326-02328*, and *ctc02331*) (Figs. 4D and 5D) were largely transcribed during Stage I and II whereas a flagellum-specific ATP synthase (*ctc01673*) (Figs. 4E and 5E) was transcribed manly during Stage I. ATPase genes, such as calcium transporter ATPases (*ctc01647, ctc02043* and *ctc02330*) were highly expressed during mid-Stage II (Figs. 4F and 5F).

2.9. Virulence factors and other related cellular programs

Transcription of genes related to virulence factors were also examined. Genes encoding for an internalin A-type protein (*ctc00494-00495*), putative PAF acetylhydrolase (*ctc00594*) and the adhesin encoding gene *slpA*/*cwp66* (*ctc00491*) showed increased expression during the first 10 h of the fermentation (Stage I) (Fig. 6A Fig. 7A). Conversely, a subset of adhesion related encoding genes (*ctc00767*, *ctc00769*, and *ctc00770-00772*) was highly expressed during Stage II of the fermentation (20 h) (Fig. 6C Fig. 7C). A distinctive expression pattern was observed for a gene encoding a periplasmic immunogenic protein (*ctc01814*); this gene showed decreasing expression towards the end of Stage I reaching its lowest value at 12 h, followed by a subsequent increased expression towards mid-late Stage II (Fig. 6B Fig. 7B). Remarkably, a subset of genes of the operon for ethanolamine uptake and degradation (*ctc02163*, *ctc02165, ctc02168, ctc02170,* and *ctc02174)* showed very similar patterns of expression (Fig. 6B Fig. 7B).

While sigma factor expression might be a response to regulatory mechanisms strictly dependent on the fermentation conditions, sporulation-related sigma factors (*ctc01125*, *ctc01126,* and *ctc01128*) were expressed during Stage II of the fermentation (Fig. 6D Fig. 7D).

2.10. Expression of the TeNT encoding plasmid pE88

The high-resolution transcriptional map of the fermentation

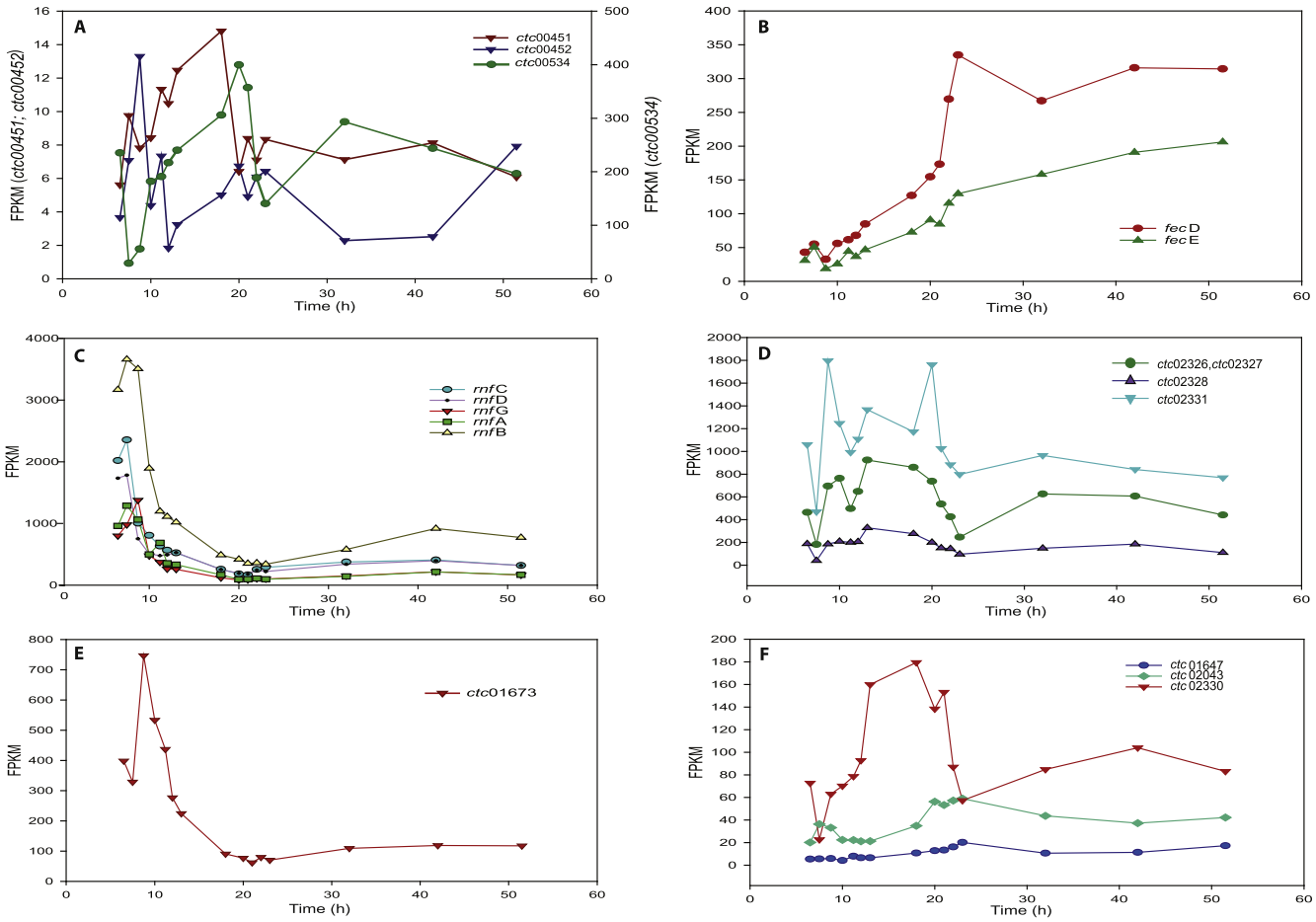

Fig. 4. Time course gene expression profile of genes belonging to iron and ATP related metabolic genes along the *C. tetani* fermentation. Transcript levels are expressed in normalized fragments per kilobase per million (FPKM) A) ferrous iron transport related genes *ctc00451-ctc00452* and *ctc00534* B) di-citrate transport system permease coding gene *fecD*|*hmuV* and hemin transport system ATP-binding protein (*fecE*) C) the Rnf Complex *rnfA-D* and *rnfG*, D) (V)-type ATP synthase coding genes *ctc02326-02328* and *ctc02331* E) flagellum-specific ATP synthase coding gene *ctc01673* and F) calcium transporter ATPase coding genes (*ctc01647*, *ctc02043* and *ctc02330*).

allowed for the full characterisation of the genes contained in the plasmid pE88. Expression levels of the gene encoding TeNT (*tetX*) and its transcriptional regulator *tetR* steadily increased (Fig. 8). Interestingly, two genes encoding for hypothetical proteins (*ctp02* and *ctp03*) showed the same expression profile to *tetR*. Other regulatory genes with relevant expression patterns during the fermentation were two putative sigma factors, encoded by *ctp10-11*; however, their expression constantly increased during the first stage of the fermentation reaching a maximum expression at 20 h. We did not find significant expression of the gene encoding the virulence factor collagenase T (*colT*).

3. Discussion

Traditional bioprocess optimisation has historically focussed on the improvement of microbial fermentation performance (*i.e.* biomass yields and final product titres), largely ignoring physiological understanding. For example, most of the industrial culture medium formulations include cost convenient carbon sources such as glucose, ignoring the fact that more suitable carbon sources could reduce undesired metabolic/physiologic effects. While developing inexpensive bioproducts is the biochemical engineer's primary goal, a compromise should be met between cost efficiency and physiological optimality for bioprocess design. Recent advances in *omics* technologies have made it possible to correlate microbial dynamic growth behaviour with transcriptional and protein expression events across the fermentation. In this study, we used a systems biology platform to correlate transcriptional events with transitional growth stages during *C. tetani* fermentation for TeNT production. We were able to identify the importance of amino acid metabolism in energy generation and biomass production. Given the nature of the complex medium used, biological replicates do not match perfectly. In fact results are similar but not identical in many cases.

Guided by transcriptomics data, the metabolic pathways for serine transport and degradation through L-serine dehydratase and threonine dehydratase leading to the production of pyruvate were mapped. Similarly, the degradation of threonine via; 1) the L-allo-threonine aldolase producing glycine and acetaldehyde or; 2) the threonine dehydratase producing ammonia and 2-oxobutanoate were identified. The data shows that the high expression of the tyrosine phenol-lyase gene (responsible for the conversion of tyrosine into phenol, pyruvate, and ammonia) supports the previous assumptions that *C. tetani* produce indole from aromatic amino acid degradation [21]. Despite these observations, it still remains unknown whether alternative tyrosine degradation pathways are active in *C. tetani* as previously reported for colonic bacteria [22].

Despite the fact that it is historically known that histidine degradation leads to the formation of glutamate via urocanate in *C. tetani* [23], only formiminoglutamase, the gene coding for the last

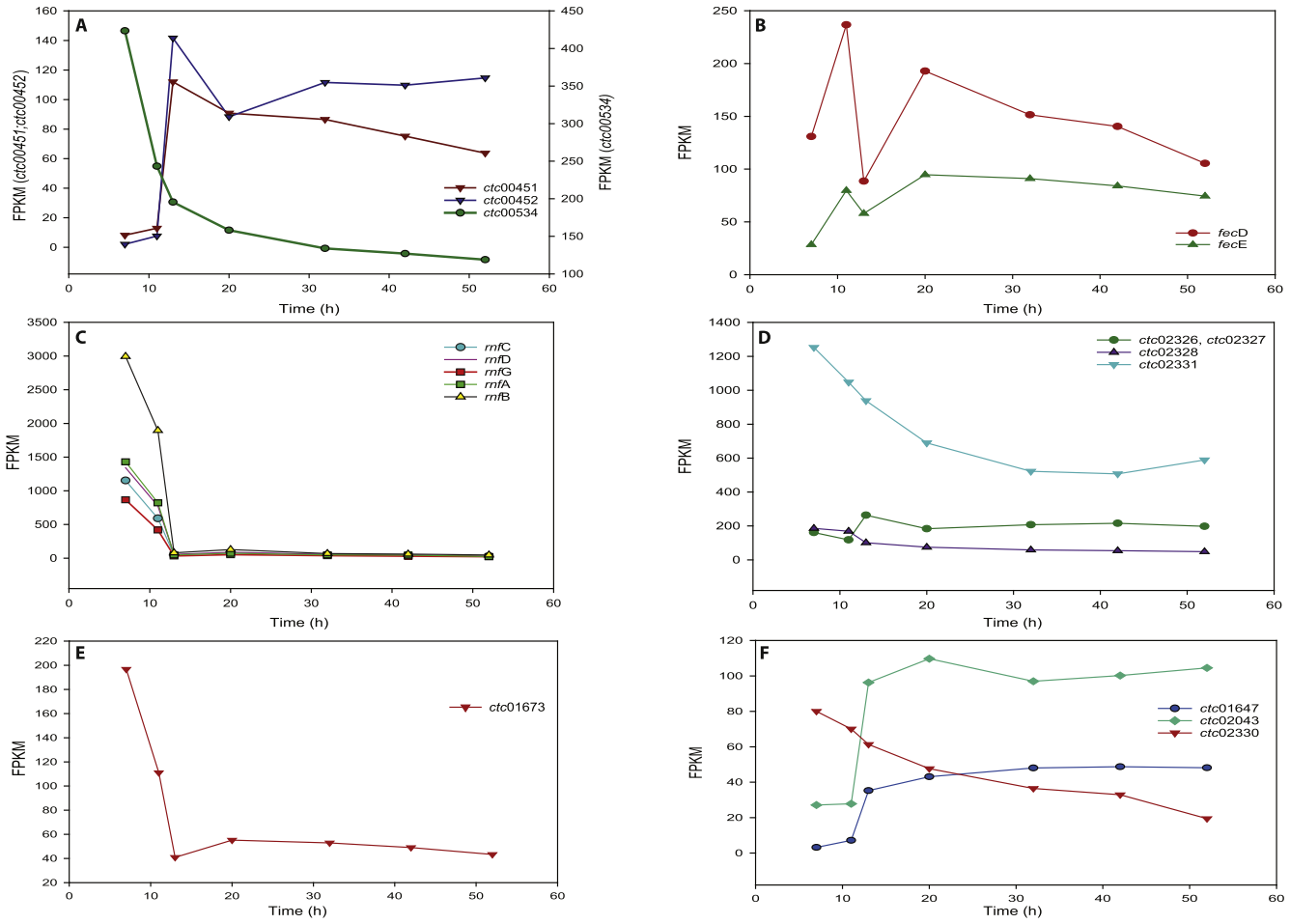

Fig. 5. Time course gene expression profile of genes belonging to iron and ATP related metabolic genes along the *C. tetani* fermentation (biological replicate). Transcript levels are expressed in normalized fragments per kilobase per million (FPKM) A) ferrous iron transport related genes *ctc00451-ctc00452* and *ctc00534* B) di-citrate transport system permease coding gene *fecD*/*hmuV* and hemin transport system ATP-binding protein (*fecE*) C) the Rnf Complex *rnfA-D* and *rnfG*, D) (V)-type ATP synthase coding genes *ctc02326-02328* and *ctc02331* E) flagellum-specific ATP synthase coding gene *ctc01673* and F) calcium transporter ATPase coding genes (*ctc01647*, *ctc02043* and *ctc02330*).

enzyme of the pathway (formiminoglutamase), was highly expressed during Stage I of the fermentation. Subsequent degradation of glutamate is likely to occur via the mesaconate pathway. The data shows that the transcriptional regulator for the methyl aspartate mutase cluster (glutamate mutase) is highly transcribed, suggesting that glutamate is catabolised to mesaconate through the cobamide-dependent pathway. While similar results were observed for *Clostridium tetanomorphum* [24], supernatant analysis from *Clostridium sticklandii* fermentations indicated accumulation of glutamate [25].

Asparagine degradation, although experimentally observed, could not be linked to any specific metabolic pathway. Transcriptomic data did not show significant expression of the L-asparaginase coding gene at any time-point of the fermentation highlighting our lack of metabolic understanding in *C. tetani*. This result shows the strong need for a functional annotation of the *C. tetani* genome based on *omics* observations (Fig. 9).

Given the importance of complex peptide mixtures (e.g. casein or peptone digests) for the biosynthesis of toxin in clostridium species, we analysed peptide consumption during *C. tetani* fermentations. Once a subset of free amino acids is consumed, peptides are degraded. An energy costly peptide transporting system is likely to be the cause of the change in growth rate from Stage I into Stage II. Similar data has been reported in casein degrading bacteria such as *Streptococcus thermophilus*. Our data shows that five casein-derived peptides are preferentially consumed. Interestingly, these peptides contain a Pro-Phe-Pro domain which has been previously reported to act as a zinc-protease inhibitor [26,27]. We consider this particularly interesting as the tetanus toxin is a zinc metalloprotease and thus, it is possible that *C. tetani* consume these peptides to block the degradation of the toxin or the activity of other zinc metalloproteases [27].

RNA-seq data shows that the expression of *tetX* and *tetR* is almost undetectable while the cells are consuming free amino acids. This was also observed when cells grew on chemically-defined medium (Supplementary Fig. 3); *tetX* and *tetR* expression increases dramatically as the cells transition from the consumption of free amino acids into the consumption of peptides. Transcriptomics confirmed that the regulator of toxin production (*tetR*) follows the same expression profile as the toxin (*tetX*) [28], along with most of the genes encoded in the plasmid and several genes linked to sporulation and this over-expression is triggered by amino acid depletion.

The homology between the botulinum and tetanus toxins suggests that they have evolved from a common ancestor. However, despite their similarity, little is known about their regulation. Moreover, BoNT toxins can be produced by different *C. botulinum* strains (serotypes from groups I to IV) with slightly different metabolic patterns and toxin regulation, whereas TeNT is produced by a homogenous group *C. tetani* [3]. Toxin production in both

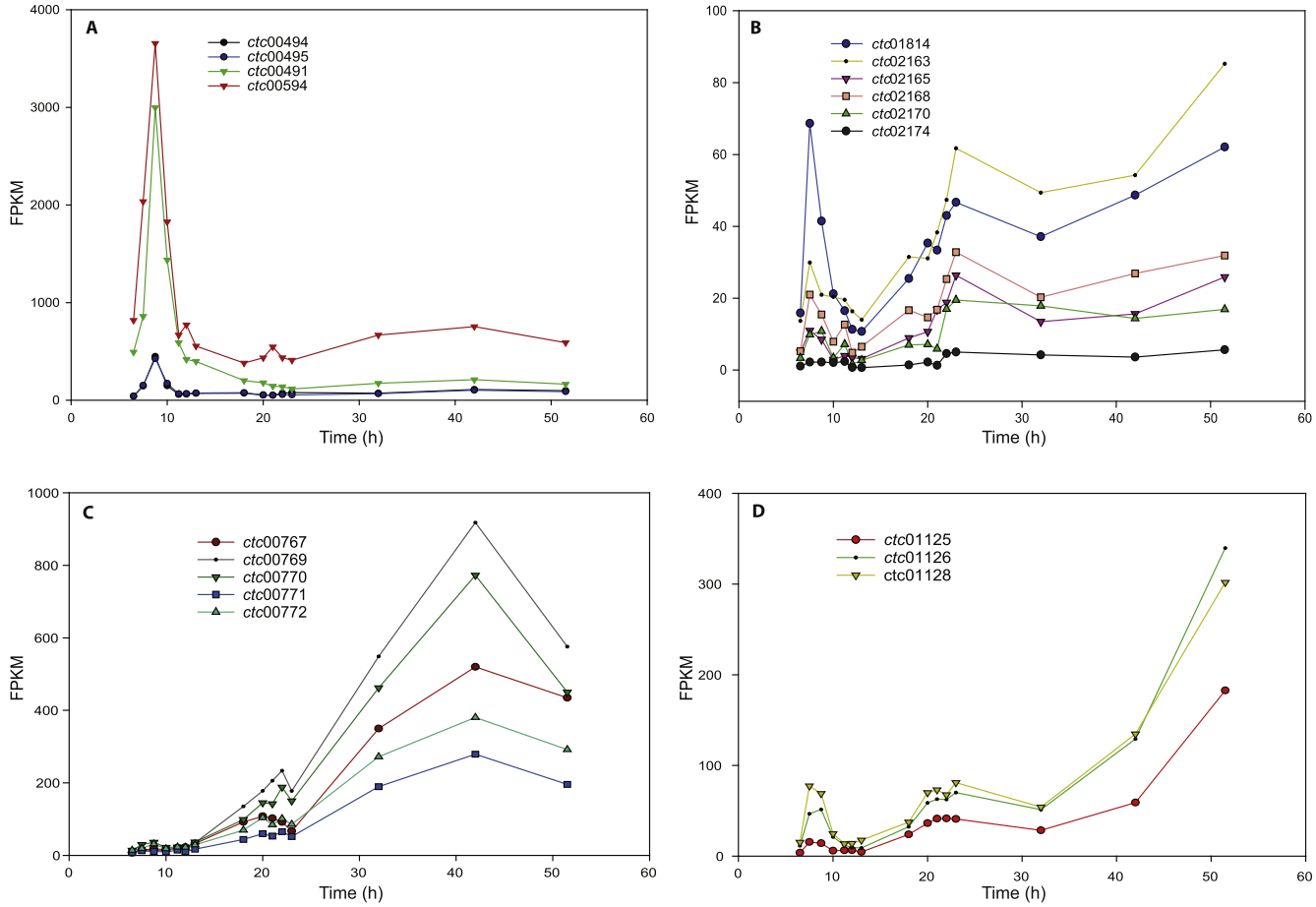

Fig. 6. Transcriptional profile of genes related to pathogenic cellular programs along the *C. tetani* fermentation. Transcript levels are expressed in normalized fragments per kilobase per million (FPKM). A) internalin A-type protein (*ctc00494-00495*), putative PAF acetylhydrolase (*ctc00594*) and adhesin encoding gene *slpA*/*cwp66* (*ctc00491*); B) periplasmic immunogenic enconding gene *ctc01814* and ethanolamine uptake and degradation genes (*ctc02163*, *ctc02165*, *ctc02168*, *ctc02170* and *ctc02174)*; C) adhesion encoding genes (*ctc00767*, *ctc00769*, *ctc00770-00772*); D) sporulation-related sigma factors (*ctc01125*, *ctc01126* and *ctc01128*).

systems is affected by culture conditions and nutritional composition of the medium. High levels of arginine, proline or glutamate in minimal medium were detrimental for the production of BoNT in *C. botulinum* Hall A and Okra B whereas the supplementation with casein increased toxin titres [29]. This seems to be also the case of *C. tetani* which consume neither arginine nor proline, in fact, proline accumulates in the medium across the fermentation. Equally, a high concentration of tryptophan lowered BoTN titre in *C. botulinum* serotype E while casein presence in the medium stimulated toxin production [30]. Glycine seems to have a stimulatory effect on the production of toxin in *C. botulinum* serotype F [31] whereas is required neither in *C. botulinum* serotype A nor in *C. tetani*. Since amino acids preference seems to be different in each organism, it is difficult to assess the nutritional requirements that govern the toxin production mechanism. Both species, however, can produce more toxin when casein is available in the medium. It is important to note that toxin regulation is not only linked to environmental signals but a more complex network where two component systems, small regulatory RNAs, quorum sensing, and environmental signals work together and interspecies correlations between our observations in *C. tetani* may be relevant to work in *C. botulinum* but need to be interpreted with extreme care as both systems are divergent in both toxin regulation and nutritional requirements.

As in other pathogens, the regulation, synthesis, and secretion of the toxin is tightly controlled by regulatory elements that are sensitive to environmental signals. Despite the enormous availability of nutrients (casein and sugar copiously available in stage IV of the fermentation), cells perform autolysis, a suicidal and seemingly non-intuitive event given the abundance of nutrients available at this stage of the process. Construction of the first molecular fermentation atlas for one of the most pharmaceutically relevant members of the clostridium family, is the first step towards the understanding of toxin biosynthesis under conditions far different from native environment. Thus, we state that a physiology-driven design of a TeNT production process in *C. tetani* is a plausible way for improving process outcomes and will have an impact on vaccine availability for humans and livestock, importantly some of our observations may be relevant to close relatives such as *C. botulinum*.

4. Materials & methods

4.1. Bacterial strain, growth and fermentation conditions

Clostridium tetani strain E88 was purchased from ATCC. Unless otherwise specified, all chemicals were purchased from Sigma (Sigma Aldrich, NSW, Australia). Seed medium 29.8 g/L of Fluid Thioglycolate (Difco, Franklin Lakes, New Jersey, USA) the inoculum seed was 500 μl and they were grown for 18 h at 37 °C. Fermentation culture medium was prepared as specified in Mueller and Miller [10] with the adjustments made by Latham et al. [9] plus the

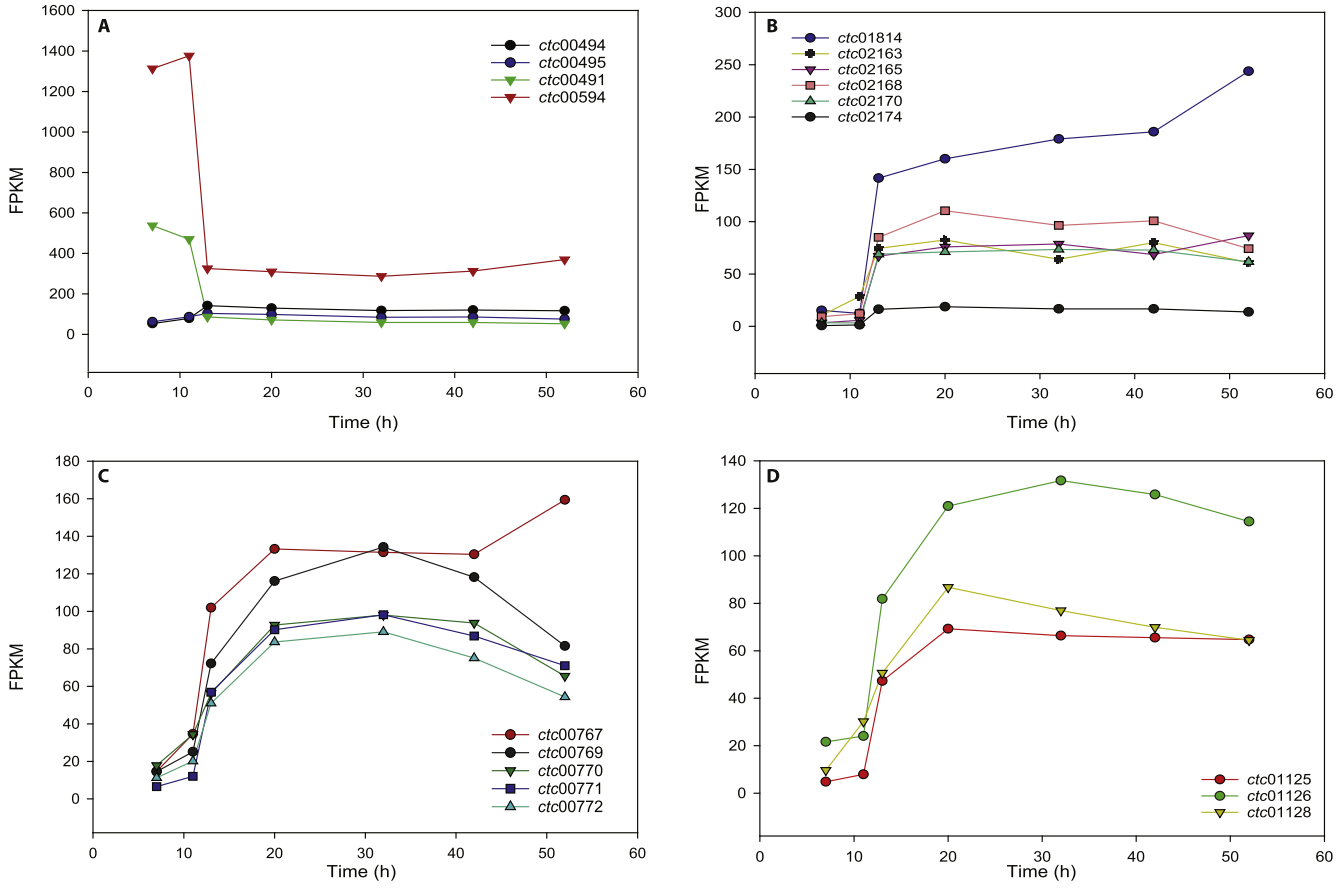

Fig. 7. Transcriptional profile of genes related to pathogenic cellular programs along the *C. tetani* fermentation (biological replicate). Transcript levels are expressed in normalized fragments per kilobase per million (FPKM). A) internalin A-type protein (*ctc00494-00495*), putative PAF acetylhydrolase (*ctc00594*) and adhesin encoding gene *slpA*/*cwp66* (*ctc00491*); B) periplasmic immunogenic enconding gene *ctc01814* and ethanolamine uptake and degradation genes (*ctc02163*, *ctc02165*, *ctc02168*, *ctc02170* and *ctc02174*); C) adhesion encoding genes (*ctc00767*, *ctc00769*, *ctc00770-00772*); D) sporulation-related sigma factors (*ctc01125*, *ctc01126* and *ctc01128*).

following modifications: 187.5 mg/L L-cystine, 0.00375 mg/L d-Biotin, 0.375 mg/L Riboflavin, Thiamine, Pyridoxine hydrochloride, and nicotinic acid; 1.5 mg/L calcium pantothenate, 0.000075 mg/L vitamin B12, 1.875 mg/L uracil, 0.03 mg/L $FeCl_3$ and N-Z-Casein. The culture medium was autoclaved at 121 °C for 18 min. The chemically defined medium was prepared as described in Ref. [18].

Samples were extracted from three different fermentations performed in 4 Multifors Infors HT bioreactors or Sartorius at working volumes of 1 and 5 L, respectively. The temperature was controlled at 35 °C throughout the fermentation. Initial anaerobic conditions were obtained by bottom sparging the medium with N_2. Post inoculation, the N_2 gassing was changed to the overlay at a rate of 340 ml/min. Four hours after the inoculation, N_2 was switched off and air was gassed into the fermenter from the overlay at a rate of 340 ml/min until the end of the fermentation.

4.2. Analytical methods

Extracellular components such as free amino acids were quantified as described in Ref. [32]. Central carbon metabolites were measured using an ion pairing HPLC-MS/MS method, as described in Ref. [33] and modified in Ref. [34]. Proteomic discovery (IDA) and quantification (SWATH) samples were first separated using a Shimadzu Prominence nano-LC system as previously described in Ref. [35] using the modifications reported by Ref. [36]. For vitamins, HPLC Grade acetonitrile and acetic acid (AR Grade) was purchased from RCI Labscan (Bangkok, Thailand) and Labscan (Gliwice, Poland), respectively. Deionised water was generated via an Elga Purelab Classic water purification unit (Veolia Water Solutions and Technologies, Saint Maurice Cedex, France). Liquid chromatography-tandem mass spectrometry (LC-MS/MS) data was acquired on a Dionex UltiMate 3000 liquid chromatography system (Dionex, California, USA) coupled to an ABSciex 4000 QTRAP mass spectrometer (ABSciex, Concord, Canada). The liquid chromatography system was controlled by Chromeleon software (v6.80 SR9, Dionex), and chromatographic separation was achieved by injecting 10 μL onto a Gemini-NX C18 150 mm × 2 mm I.D., 3 μm 110 Å particle column (Phenomenex, Aschaffenburg, Germany) equipped with a pre-column Security Guard Gemini-NX C18 4 mm × 2 mm I.D. cartridge. The column oven temperature was controlled and maintained at 55 °C throughout the acquisition and the mobile phases, adapted from Refs. [37], were as follows: 7.5 mM aqueous tributylamine adjusted to pH 4.95 (±0.05) with glacial acetic acid (eluent A) and acetonitrile (eluent B). The mobile phase flow rate was maintained at 300 μL/min throughout the gradient profile (Supporting Table 2) and was introduced directly into the mass spectrometer with no split. The mass spectrometer was controlled by Analyst 1.5.2 software (ABSciex) and was equipped with a TurboV electrospray source operated in negative ion mode. The following optimised parameters were used to acquire scheduled Multiple Reaction Monitoring (MRM) data: ionspray voltage −4500 V, nebulizer (GS1), auxiliary (GS2), curtain (CUR) and collision (CAD) gases were 60, 60, 20 and medium (arbitrary units), respectively. The auxiliary gas temperature was maintained

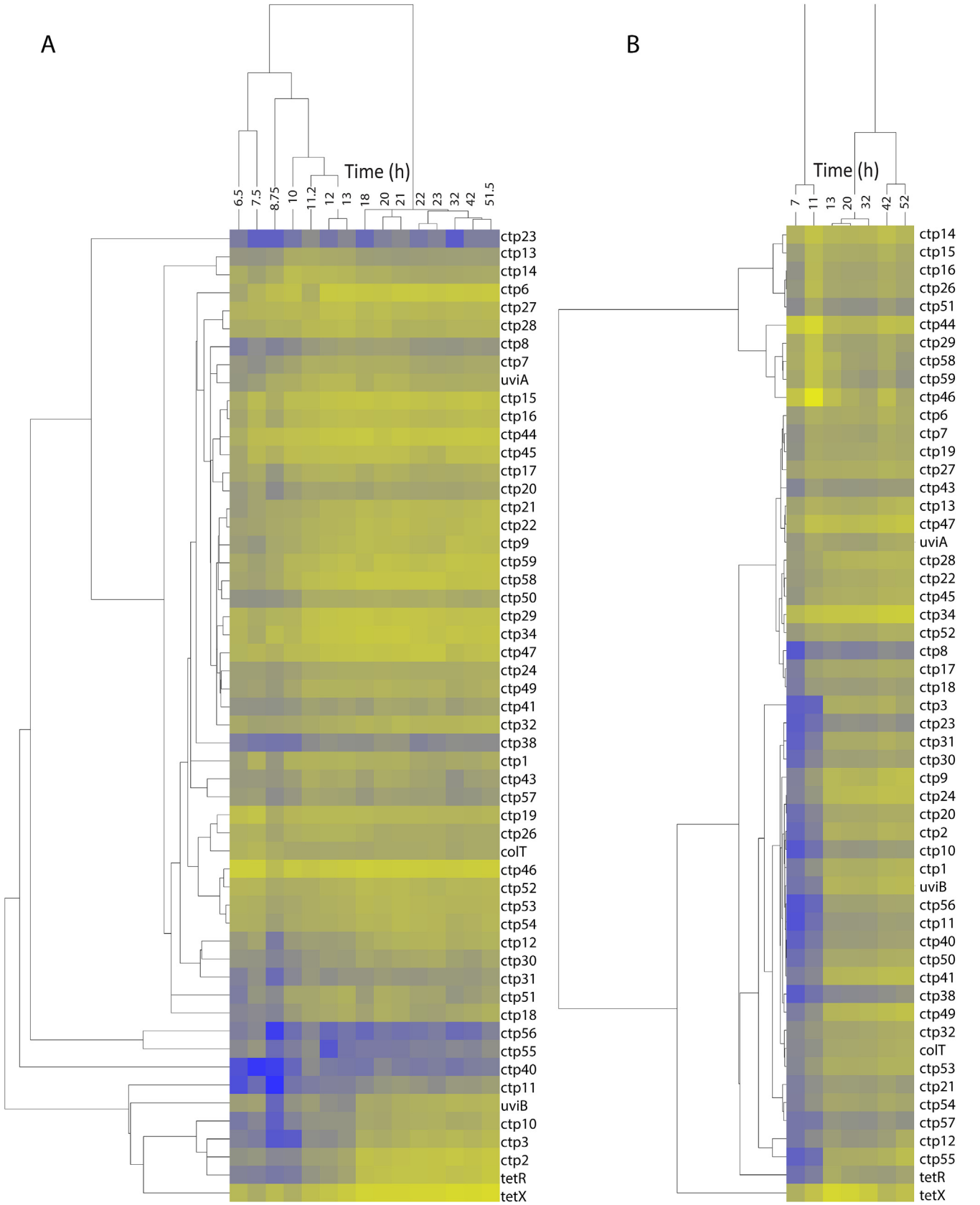

Fig. 8. A and B show heat maps for all genes encoded in the pe88 Plasmid. As shown in the heat-map, most genes encoded in the plasmid display a similar transcriptional profile as the genes *tetX* and *tetR* in both fermentations.

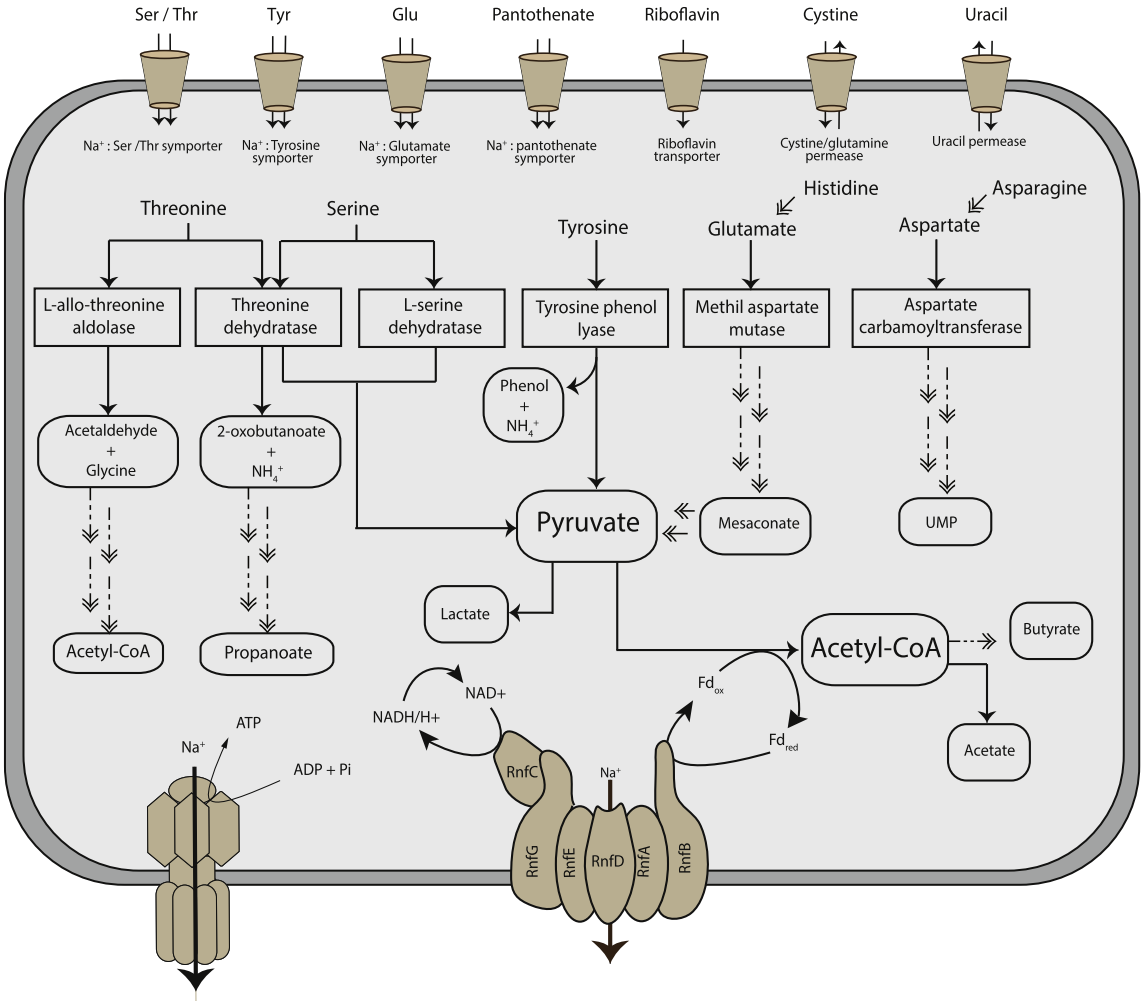

Fig. 9. Central carbon metabolic pathways for *C. tetani*. The Fig illustrates the pathways involved in amino acid transport, catabolism and ATP metabolism. *tetX* and *tetR* expression increase dramatically as the cells transition from the consumption of free amino acids into the consumption of peptides, showing that amino acids catabolism plays a key role in virulence in *C. tetani.*

at 350 °C. For all analytes the entrance potential (EP) was −10 V. The samples were run with sample- and analyte-relevant calibration standards and pooled QC samples [38,39] to control for reproducibility of data acquisition and to ensure data integrity. Analyte stock solutions were prepared in purified water (Veolia) and aliquots of each solution were mixed to achieve a final calibrant solution at 50 μM. This calibrant solution was serially diluted and the dilutions used as calibration standards from 50 to 0.195 μM, constituting $5 \leq x \leq 9$ calibration points to account for differential responses in the mass spectrometer. As an internal standard, 1 μl of a 1 mM aqueous solution of azidothymidine was added to 99 μL of sample. Data were processed using MultiQuant 2.1 software (ABSciex).

SWATH samples were prepared as specified in Ref. [40]. Briefly, 50 μg of casein was diluted in 800 μL of 8 M urea/50 mM AMBIC and loaded into four Amicon Ultra-0.5 ml centrifugal filters with nominal cut-off of 30,000 Da (Millipore). Protein samples were washed twice with 200 μL of 8 M urea/50 mM AMBIC by centrifugation (14,000 g for 15 min), followed by two washes in 100 μL of 50 mM AMBIC. In-filter trypsin digestion was performed (overnight at 37 °C, 50 rpm) using 5 μg of MS-grade trypsin (Promega) in 30 μL of AMBIC (50 mM). Digested proteins were collected by three rounds of centrifugation with 30 μL of AMBIC (50 mM). Final pH of the samples was adjusted to 3 using formic acid, concentrated using a vacuum centrifuge, and finally concentrated using a C-18 ZipTip (Millipore) to assure equal quantities were injected in each LC injection. Information-Dependent Acquisition (IDA) was used to generate a reference library from a pooled sample that included 50 μg of proteins from each of time points across the fermentation in two biological replicates. In order to avoid column overloading, C-18 ZipTips were used. Prior to MS analysis, samples were concentrated using a vacuum centrifuge to remove residual acetonitrile (ACN) and resuspended in 99.5 μL of 0.1% formic acid. Synthetic peptide mixture (HRM calibration kit from Biognosys) was spiked to each sample for retention time shift correction according to [41]. IDA and SWATH injections were injected by duplicate from 4 μg of peptides and from 0.5 μg of peptides, respectively.

4.3. RNA isolation, mRNA enrichment, RNASeq sequencing

Total RNA was extracted from *C. tetani* with RNeasy midi column as per manufacturer's instructions plus the addition of a mechanical disruption through a bead beating step and the off-column DNase I treatment. RNA quality was evaluated using BioAnalyzer (Agilent) and Nanodrop 1000 (Thermo Scientific). Ribosomal RNA was removed using the ribo-zero meta-bacterial kit (Epicentre). mRNA libraries for sequencing were prepared using TruSeq RNA

sample preparation kits from Illumina. All sequencing was performed at the University of Queensland on the Illumina Hiseq-2000.

4.4. Transcriptomic analysis

Reads were aligned to the genome using TopHat [42], with two mismatches allowed per read alignment. Before mapping to the genome the 100 bp reads were trimmed to 75 bp to avoid reading errors. Transcript abundance was estimated using FPKM from cufflinks [43] using classic-FPKM normalisation, CuffDiff was used to estimate differentially expressed proteins. A log2-fold change of + 2 or - 2 and 0.05 false discovery rate was used to estimate significant changes. Transcript data were also assessed globally by Principal Component Analysis, and correlation with the fermentation time course further analysed by Partial Least Squares/Projection to Latent Structures (PLS) and Orthogonal PLS using SIMCA (version 13.0.3.0; MKS Umetrics AB, Umea, Sweden).

Acknowledgments

This paper was funded through LP150100087. The authors would like to thank Amanda Nouwens from the SCMB proteomics facility for assistance with LCMS injections, Manuel Plan for HPLC analyses and Robin W. Palfreyman for RNA-seq alignment processing.

Conflict of interest

Zoetis has interest in commercializing Tetanus vaccines.

Appendix A. Supplementary data

Supplementary data related to this article can be found at http://dx.doi.org/10.1016/j.anaerobe.2016.07.006.

References

[1] T.M. Cook, R.T. Protheroe, J.M. Handel, Tetanus: a review of the literature, Br. J. Anaesth. 87 (2001) 477–487.
[2] F.C. Blum, C. Chen, A.R. Kroken, J.T. Barbieri, Tetanus toxin and botulinum toxin a utilize unique mechanisms to enter neurons of the central nervous system, Infect. Immun. 80 (2012) 1662–1669.
[3] C. Connan, C. Deneve, C. Mazuet, M.R. Popoff, Regulation of toxin synthesis in *Clostridium botulinum* and *Clostridium tetani*, Toxicon official J. Int. Soc. Toxinology 75 (2013) 90–100.
[4] C. Grumelli, C. Verderio, D. Pozzi, O. Rossetto, C. Montecucco, M. Matteoli, Internalization and mechanism of action of clostridial toxins in neurons, Neurotoxicology 26 (2005) 761–767.
[5] B. Bizzini, Tetanus toxin, Microbiol. Rev. 43 (1979) 224–240.
[6] I. Brook, Current concepts in the management of Clostridium tetani infection, Expert Rev. Anti Infect. Ther. 6 (2008) 327–336.
[7] T. Binz, A. Rummel, Cell entry strategy of clostridial neurotoxins, J. Neurochem. 109 (2009) 1584–1595.
[8] F. Fratelli, T.J. Siquini, S.M.A. Prado, H.G. Higashi, A. Converti, J.C.M. de Carvalho, Effect of medium composition on the production of tetanus toxin by *Clostridium tetani*, Biotechnol. Prog. 21 (2005) 756–761.
[9] W.C. Latham, D.F. Bent, L. Levine, Tetanus toxin production in the absence of protein, Appl. Microbiol. 10 (1962) 146–152.
[10] J.H. Mueller, P.A. Miller, Variable factors influencing the production of tetanus toxin, J. Bacteriol. 67 (1954) 271–277.
[11] H. Jing, D.D. Kitts, Chemical characterization of different sugar-casein Maillard reaction products and protective effects on chemical-induced cytotoxicity of Caco-2 cells, Food Chem. Toxicol. 42 (2004) 1833–1844.
[12] B. Zacharias, M. Bjorklund, Continuous production of Clostridium tetani toxin, Appl. Microbiol. 16 (1968) 69–72.
[13] F. Fratelli, T.J. Siquini, M.E. de Abreu, H.G. Higashi, A. Converti, J.C.M. de Carvalho, Fed-batch production of tetanus toxin by *Clostridium tetani*, Biotechnol. Prog. 26 (2010) 88–92.
[14] J.C. Marvaud, U. Eisel, T. Binz, H. Niemann, M.R. Popoff, TetR is a positive regulator of the tetanus toxin gene in *Clostridium tetani* and is homologous to BotR, Infect. Immun. 66 (1998) 5698–5702.
[15] G.P. Carter, J.K. Cheung, S. Larcombe, D. Lyras, Regulation of toxin production in the pathogenic clostridia, Mol. Microbiol. 91 (2014) 221–231.
[16] G.K. Bergey, W.H. Habig, J.I. Bennett, C.S. Lin, Proteolytic cleavage of tetanus toxin increases activity, J. Neurochem. 53 (1989) 155–161.
[17] J. Nielsen, M.C. Jewett, Impact of systems biology on metabolic engineering of *Saccharomyces cerevisiae*, FEMS Yeast Res. 8 (2008) 122–131.
[18] I. Vanderijn, R.E. Kessler, Growth-characteristics of group-a Streptococci in a new chemically defined medium, Infect. Immun. 27 (1980) 444–448.
[19] J. Trygg, E. Holmes, T. Lundstedt, Chemometrics in metabonomics, J. Proteome Res. 6 (2007) 469–479.
[20] M. Bylesjo, M. Rantalainen, O. Cloarec, J.K. Nicholson, E. Holmes, J. Trygg, OPLS discriminant analysis: combining the strengths of PLS-DA and SIMCA classification, J. Chemom. 20 (2006) 341–351.
[21] H.A. Barker, Aminoacid degradation by anaerobic bacteria, Annu. Rev Biochem. 50 (1981) 23–40.
[22] E.A. Smith, G.T. Macfarlane, Formation of phenolic and indolic compounds by anaerobic bacteria in the human large intestine, Microb. Ecol. 33 (1997) 180–188.
[23] M.J. Pickett, Studies on the metabolism of *Clostridium tetani*, J. Biol. Chem. 151 (1943) 203–209.
[24] W. Buckel, H.A. Barker, 2 Pathways of glutamate fermentation by anaerobic bacteria, J. Bacteriol. 117 (1974) 1248–1260.
[25] N. Fonknechten, S. Chaussonnerie, S. Tricot, A. Lajus, J.R. Andreesen, N. Perchat, et al., Clostridium sticklandii, a specialist in amino acid degradation: revisiting its metabolism through its genome sequence, BMC Genomics 11 (2010).
[26] A. Quiros, M. Ramos, B. Muguerza, M.A. Delgado, M. Miguel, A. Aleixandre, et al., Identification of novel antihypertensive peptides in milk fermented with, Enterococcus Faecalis. Int. Dairy J. 17 (2007) 33–41.
[27] Z. Porfirio, S.M. Prado, M.D.C. Vancetto, F. Fratelli, E.W. Alves, I. Raw, et al., Specific peptides of casein pancreatic digestion enhance the production of tetanus toxin, J. Appl. Microbiol. 83 (1997) 678–684.
[28] J.C. Marvaud, U. Eisel, T. Binz, H. Niemann, M.R. Popoff, TetR is a positive regulator of the tetanus toxin gene in Clostridium tetani and is homologous to BotR, Infect. Immun. 66 (1998) 5698–5702.
[29] S.I. Patterson-Curtis, E.A. Johnson, Regulation of neurotoxin and protease formation in Clostridium botulinum Okra B and Hall A by arginine, Appl. Environ. Microbiol. 55 (1989) 1544–1548.
[30] G.J. Leyer, E.A. Johnson, Repression of toxin production by tryptophan in Clostridium botulinum type E, Arch. Microbiol. 154 (1990) 443–447.
[31] L.V. Holdeman, L.D. Smith, Study of the nutritional requirements and toxin production of Clostridium botulinum type F, Can. J. Microbiol. 11 (1965) 1009–1019.
[32] S. Dietmair, N.E. Timmins, P.P. Gray, L.K. Nielsen, J.O. Kromer, Towards quantitative metabolomics of mammalian cells: development of a metabolite extraction protocol, Anal. Biochem. 404 (2010) 155–164.
[33] S. Dietmair, M.P. Hodson, L.-E. Quek, N.E. Timmins, P. Gray, L.K. Nielsen, A multi-omics analysis of recombinant protein production in Hek293 cells, PloS One 7 (2012) e43394.
[34] T.S. McDonald, K.N. Tan, M.P. Hodson, K. Borges, Alterations of hippocampal glucose metabolism by even versus uneven medium chain triglycerides, J. Cereb. Blood Flow. Metab. 34 (2014) 153–160.
[35] U. Kappler, A.S. Nouwens, The molybdoproteome of *Starkeya novella* - insights into the diversity and functions of molybdenum containing proteins in response to changing growth conditions, Metallomics 5 (2013) 325–334.
[36] C.A. Orellana, E. Marcellin, B.L. Schulz, A.S. Nouwens, P.P. Gray, L.K. Nielsen, High-antibody-producing chinese hamster ovary cells up-regulate intracellular protein transport and glutathione synthesis, J. proteome Res. 14 (2015) 609–618.
[37] B. Luo, K. Groenke, R. Takors, C. Wandrey, M. Oldiges, Simultaneous determination of multiple intracellular metabolites in glycolysis, pentose phosphate pathway and tricarboxylic acid cycle by liquid chromatography–mass spectrometry, J. Chromatogr. A 1147 (2007) 153–164.
[38] T. Sangster, H. Major, R. Plumb, A.J. Wilson, I.D. Wilson, A pragmatic and readily implemented quality control strategy for HPLC-MS and GC-MS-based metabonomic analysis, Analyst 131 (2006) 1075–1078.
[39] M. Hodson, G. Dear, J. Griffin, J. Haselden, An approach for the development and selection of chromatographic methods for high-throughput metabolomic screening of urine by ultra pressure LC-ESI-ToF-MS, Metabolomics 5 (2009) 166–182.
[40] J.R. Wisniewski, A. Zougman, N. Nagaraj, M. Mann, Universal sample preparation method for proteome analysis, Nat. Methods 6 (2009) 359–362.
[41] C. Escher, L. Reiter, B. MacLean, R. Ossola, F. Herzog, J. Chilton, et al., Using iRT, a normalized retention time for more targeted measurement of peptides, Proteomics 12 (2012) 1111–1121.
[42] B. Langmead, S.L. Salzberg, Fast gapped-read alignment with Bowtie 2, Nat. Methods 9 (2012), 357–U54.
[43] C. Trapnell, B.A. Williams, G. Pertea, A. Mortazavi, G. Kwan, M.J. van Baren, et al., Transcript assembly and quantification by RNA-Seq reveals unannotated transcripts and isoform switching during cell differentiation, Nat. Biotechnol. 28 (2010) 511–515.